연구논문

J Korean Soc Fluid Power Constr Equip Vol.11 No.1 pp.14-24 Mar. 2014
ISSN(print) 2234-8328 ISSN(online) 2287-6146
http://dx.doi.org/10.7839/ksfc.2014.11.1.014

엔진윤활용 가변 베인펌프의 수학적 모델 해석
Analysis of the Mathematical Model of a Variable Displacement Vane Pump for Engine Lubrication

딩광청[1] · 안경관[1*] · 이재신[2]
D. Q. Truong, K. K. Ahn and J. S. Lee

Received: 7 Jan. 2014, Revised: 22 Feb. 2014, Accepted: 25 Feb. 2014

Key Words : Engine Lubrication(엔진윤활), Vane Pump(베인펌프), Variable Displacement(가변용량), Modeling (모델링)

Abstract: Variable displacement vane-type oil pumps represent one of the most innovative pump types for industrial applications, especially for engine lubrication systems. This paper presents a complete and accurate mathematical model for a typical variable displacement vane-type oil pump. Firstly, its theoretical model is revised. Secondly, an analysis of power loss factors of this pump type is carefully investigated to optimize the modeling accuracy. Finally, the estimated pump performance using the complete pump model is verified by numerical simulations in comparison with the practical tests.

1. Introduction

In recent years, the design requirements for engine lubrication systems, especially for vehicle applications, have been oriented to a general performance improvement, coupled with a contemporary reduction of power losses, weights and volumes. A fixed displacement lubricating pump is generally operates effectively at a target speed and a maximum operating lubricant temperature. Meanwhile, the lubrication requirements of the machine do not directly correspond to its operating speed. It results in an oversupply of lubricating oil at most machines. A pressure relief valve is then provided to return the surplus lubricating oil back into the pump inlet or a reservoir to avoid over pressure conditions in the mechanical system. The result is a significant amount of energy being used to pressurize the lubricating oil which is subsequently exhausted through the relief valve. Subsequently, a potential trend for machine lubrication is the employment of variable displacement vane pumps as lubrication oil pumps. To vary the displacement, there are two common approaches which are the use of a linear translating cam ring1-3), and the use of a pivoting cam ring[4-12]. By the second method, each pump generally includes a control ring combined with other mechanisms such as springs, which can be operated to alter the volumetric displacement of the pump and thus its output at an operating speed. The pump control mechanisms are normally supplied with pressurized lubricating oil from the pump output to drive the pump displacement and to avoid over pressure situations in the engine throughout the expected operating range of the mechanical system. Therefore, development of a

* Corresponding author: kkahn@ulsan.ac.kr
1 School of Mechanical Engineering, University of Ulsan, Ulsan, Korea.
2 School of Materials Science and Engineering, University of Ulsan, Ulsan, Korea.

variable displacement vane-type oil pump model is indispensable and can be considered as a priority task in order to investigate the pump working performance as well as to optimize the pump design structure. Some studies relating to this field have been done to investigate the pump performances[8-11]. Giuffrida and Lanzafame[8] derived a mathematical model for a fixed displacement balanced vane pump to analyze the theoretical flow rate through the cam shape design and vane thickness. Staley et al.[9] carried out a study on a variable displacement vane pump for engine lubrication. Loganathan et al.[10] also developed a variable displacement vane pump for automotive applications by simulations and experiments. In another study, Kim et al.[11] investigated an electronic control variable displacement lubrication oil pump through a simple mathematical model. Although these studies bring some interesting results, a detailed analysis of the theoretical performance as well as a careful investigation on the power losses of a variable displacement vane-type oil pump in order to derive an accurate model based on practical experiments was not considered.

This paper is to investigate carefully the power loss factors of the actual pump during its operation. It is based on the pump geometric and dynamic analyses, and its theoretical model developed by the authors in the previous work[13]. As a result, the actual pump performance can be estimated well by using this model. It can be considered as mandatory steps for a deeper understanding of pump operation as well as for effectively implementing pump control mechanism to satisfy the urgent lubrication demands.

2. Overview of The Researched Vane Pump and Its Theoretical Model

2.1 The researched vane type oil pump

In this study, a variable displacement vane-type oil pump made by MyungHwa Co. Ltd.[11] as displayed in Fig. 1 was used for the investigation. During the pump operation, the vanes slide out of the rotor slots and the vane tip-edges always contact with the ring inside contour due to their centrifugal effects. Subsequently, it performs pumping chambers between succeeding vanes to carry oil from the inlet to the outlet. The increase in volumes forming by pumping chambers allows the oil to be pushed in by atmospheric pressure from oil sump through suction pipe.

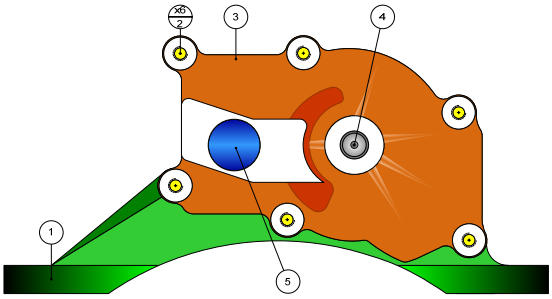

(a) Outside view of the pump

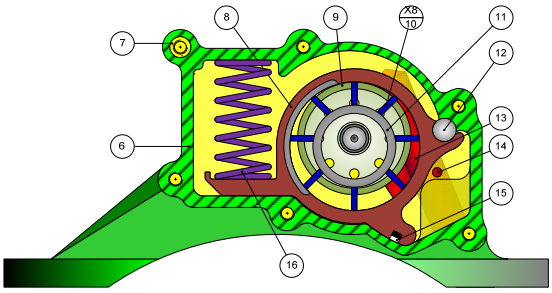

(b) Internal structure of the pump

1 Base	6 Main-covered coat	11 Sub ring
2 Tapped holes	7 Located pin	12 Pivot pin
3 Sub-covered coat	8 Main ring	13 Deliver port
4 Drive shaft	9 Rotor	14 Orifice
5 Suction port	10 Vanes	15 Oil seals
		16 Spring

Fig.1 The vane type oil pump for research

The pumping chamber volumes continue to increase in size for the first half of each rotation. The oil is then carried to the other side where the pumping chamber volumes begin to be reduced. Finally, the oil is squeezed out at the outlet as the pumping chamber's size decreases. For varying the pump displacement, rotation of the main ring around the pivot pin is controlled by pressurized oil itself in the control chamber through the orifice, the pumping chambers, centrifugal force effects and the return spring.

From the previous results[13], the pump

theoretical model is presented in Section 2.2.

2.2 Pump theoretical model

2.2.1 Flow rate analysis

The analysis of a generic vane i^{th} is carried out on a cross section of the pump as in Fig. 2. Points O_r and O_s are in turn the centers of rotor and main ring inside surface of which their radii are R_r and R_s. The eccentricity between the rotor and the ring inner surface is e_c. There are N vanes with thickness t_v and radius R_v at its tip curve (center point O_{vi}). The rotor rotates with a constant velocity ω (pump speed is n).

The vane lift (l_v) can be obtained as

$$l_{vi} = \overline{O_r B_i} - R_r = \overline{O_r O_{vi}} + R_v - R_r \tag{1}$$

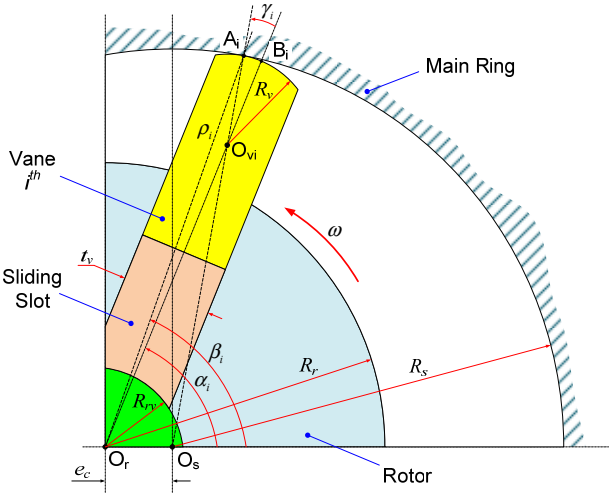

Fig. 2 Geometric analysis of a generic vane

For a small rotational angle of the rotor $d\alpha$, the volume derivative of the chamber under vane i^{th} is $dV_{uv}(\alpha_i)/d\alpha$ and, the volume derivative of a chamber between two consecutive vanes (i^{th} and $(i+1)^{\text{th}}$) is $dV_{bv}(\alpha_i,\alpha_{i+1})/d\alpha$. Then the theoretical flow rate of the pump can be computed as

$$\begin{aligned} Q_{th}(\alpha) = &\frac{1}{2}\omega\sum_{i=1}^{N}\frac{dV_{uv}(\alpha_i)}{d\alpha}\left[sign\left(dV_{uv}(\alpha_i)\right)-1\right] \\ &+\frac{1}{2}\omega\sum_{i=1}^{N-1}\frac{dV_{bv}(\alpha_i,\alpha_{i+1})}{d\alpha}\left[sign\left(dV_{bv}(\alpha_i,\alpha_{i+1})\right)-1\right] \\ &+\frac{1}{2}\omega\frac{dV_{bv}}{d\alpha}(\alpha_N,\alpha_1)\left[sign\left(dV_{bv}(\alpha_N,\alpha_1)\right)-1\right] \end{aligned} \tag{2}$$

2.2.2 Main ring rotation analysis

a) Force due to pressurized oil inside main ring

Total moment acting on the ring caused by the pressurized oil inside the ring can be computed as the bellow equation (Fig. 3):

$$\begin{aligned} \sum M_{O_{p\_oil\_inside}} = &\int_0^{\alpha_{C2t}} R_{rot}\sin(\psi_{st}+\alpha_s)P_{\min}bR_s d\alpha_s \\ &+\int_{\alpha_{C2t}}^{\alpha_{C3t}} R_{rot}\sin(\psi_{st}+\alpha_s) \\ &\times\left[(P_{\max}-P_{\min})\frac{\alpha_s-\alpha_{C2t}}{\alpha_{C3t}-\alpha_{C2t}}+P_{\min}\right]bR_s d\alpha_s \\ &+\int_{\alpha_{C3t}}^{2\pi} R_{rot}\sin(\psi_{st}+\alpha_s)P_{\max}bR_s d\alpha_s \end{aligned} \tag{3}$$

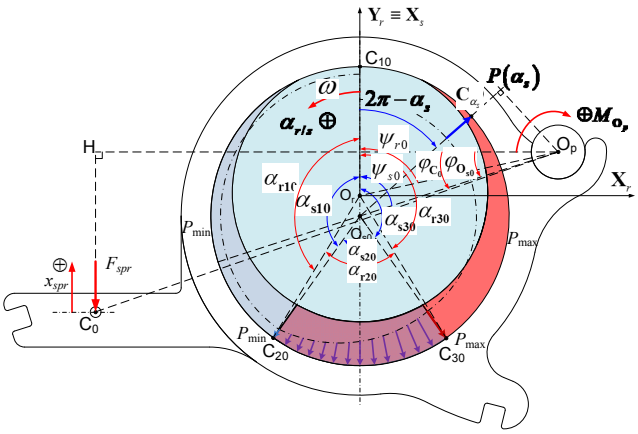

(a) At initial position of main ring

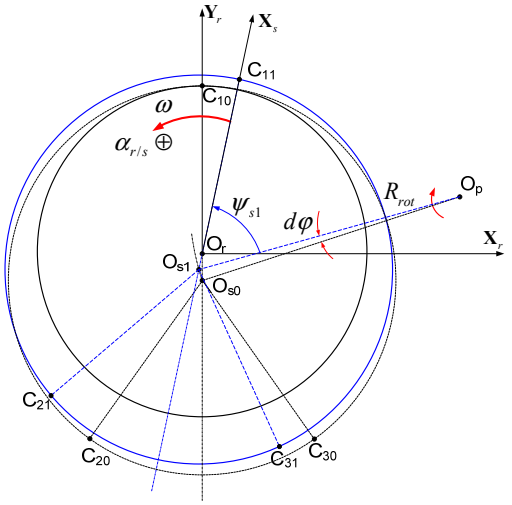

(b) After a small rotation of main ring

Fig. 3 Pressure distribution inside main ring

b) Force due to pressurized oil outside main ring (through the control orifice)

Total moment acting on the ring outer surface caused by the pressurized oil is derived (see Fig. 4)

$$\begin{aligned}\sum M_{O_{p\_oil\_outside}} &= \int_{\mu_{1a}}^{\mu_{1b}} \overline{O_pO_1}\sin\mu P_{out} b R_1 d\mu \\ &+ \int_{\mu_{3a}}^{\mu_{3b}} \overline{O_pO_3}.\sin\mu P_{out} b R_3 d\mu \\ &- \int_{\mu_{2a}}^{\mu_{2b}} \overline{O_pO_2}\sin\mu P_{out} b R_2 d\mu \\ &- \int_{\mu_{4a}}^{\mu_{4b}} \overline{O_pO_4}\sin\mu P_{out} b R_4 d\mu \end{aligned} \quad (4)$$

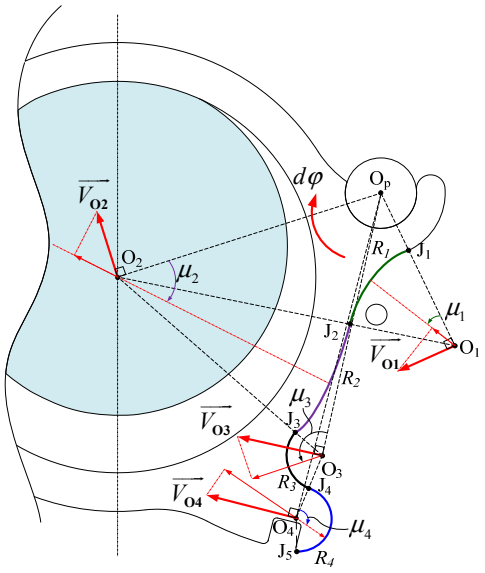

(a) Motion analysis of main ring

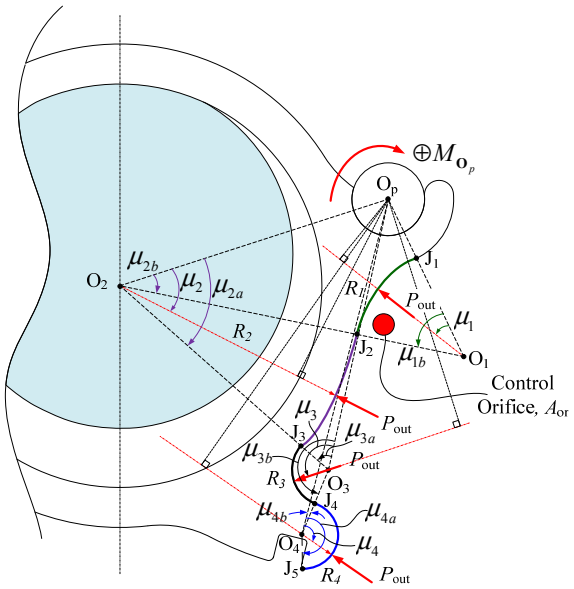

(b) Pressure analysis at outside chamber

Fig. 4 Pressure distribution outside main ring

c) *Force due to centrifugal effects of vanes and oil volumes between vanes*

Here, centrifugal forces are due to oil volume between vanes, oil volumes under vanes and vanes. The centrifugal force generated by an oil chamber between each two consecutive vanes is analyzed in Fig. 5. Then, the centrifugal force of an object of mass m_i travelling in a circle with radius $R(m_i)$ around the rotor center can be presented as in Fig. 6. From this analysis, total moment acting on the ring caused by the centrifugal forces of N vanes and N oil chambers:

$$\sum M_{O_{p\_cen}} = -\sum_{i=1}^{N} F_{cen}(m_i)\times\cos\left(\delta(m_i)\right)\times\overline{O_pM_i} \quad (5)$$

$$\overline{O_pM_i} = \sqrt{\overline{O_pO_r}^2 + R^2(m_i) - 2\overline{O_pO_r}R(m_i)\cos\left(\alpha_r(m_i)+\psi_r\right)} \quad (6)$$

$$\delta(m_i) = \frac{\pi}{2} + \text{asin}\left[\frac{\overline{O_pO_r}}{\overline{O_pM_i}}\sin\left(\alpha_r(m_i)+\psi_r\right)\right] \quad (7)$$

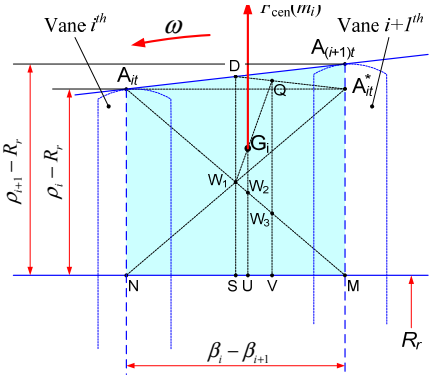

Fig. 5 Centrifugal force generated by an oil

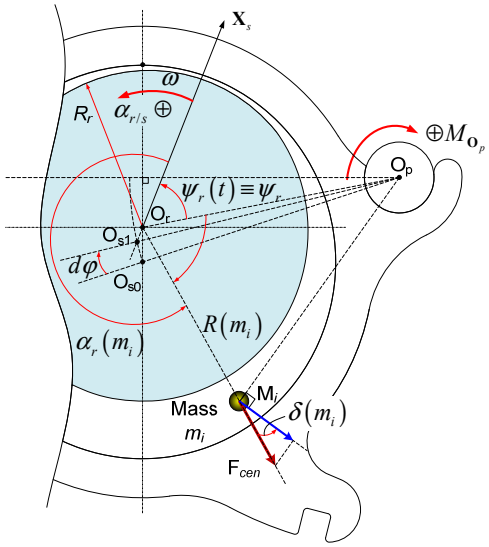

Fig. 6 Centrifugal force effect on ring rotation

d) *Force of compression spring*

From Fig. 3, the moment generated by the spring force can be computed as

$$M_{O_{spr}} = -F_{spr} \times \overline{O_p H} \cos(\varphi_C) \tag{8}$$

where F_{spr} is derived as

$$F_{spr} = F_{spr0} + k_{spr} x_{spr};$$
$$\left(F_{spr0} \text{ is pre-load force of the spring at initial position}\right) \tag{9}$$

Finally, the ring rotation defined by summing moments acting on the ring around the pivot point:

$$I_{ring}\ddot{\varphi} = \sum M_{O_{p\_oil\_inside}} + \sum M_{O_{p\_oil\_outside}} + \sum M_{O_{p\_cen}} + M_{O_{spr}} \tag{10}$$

here I_{ring} is the ring moment of inertia.

3. Actual Power Loss Analysis

3.1 Experimental analysis

To investigate the actual performance of the vane pump, an apparatus has been setup as in Fig. 7. The system hardware mainly includes the pump driven by an AC servo motor, a flow control valve, a thermo regulator, an oil sump and proper sensors. The system control part includes an electric control box and a compatible PC. During the operation, the pump speed is ensured by the motor while the pump flow rate is adjusted by the fabricated actuator. The lubrication oil used for experiments was SAE 5W-20 series.

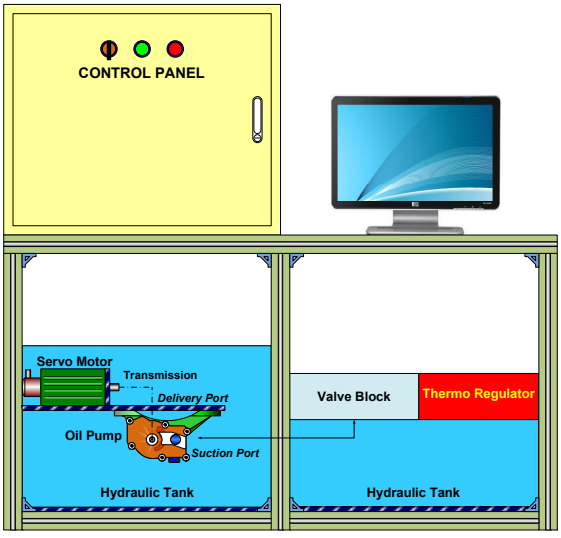

Fig. 7 Experimental apparatus

The load and oil conditions are created by the flow control valve and thermo regulator, respectively. For evaluating the system, torque and speed sensors are used to measure the driving torque and speed of the pump while pressure gauge and flow meter are used to measure the pump output pressure and flow rate. To ensure the suitable oil level of the oil sump during the tests, lever switch sensors are employed. To represent as the real lubrication conditions, the fixed flow restriction valve was employed. For the experiments, the pump speed was varied from 0 to 4000rpm with a step of 500rpm while the valve opened area was set to 60%. The working temperature during these experiments was controlled to be constant at 120°C by using a thermo regulating system. The experimental results were then obtained as shown in Fig. 8. From this figure, it can be seen that the actual pump flow rate is largely different with the theoretical flow rate[13]. The reason for it is the loss of power during the system operation.

3.2 Actual power loss analysis

3.2.1 Power loss due to leakages

Internal leakage is generally caused by the pressure distribution within the pump and the clearances associated with the pumping chambers. Because the volumes of chambers under vanes are significantly small in comparison with those of chambers between vanes, the leakage flows are only investigated with chambers between vanes.

For a generic chamber between two consecutive vanes represented by the angles$(\alpha_1,\ \alpha_{i+1})$. There are 8 leakage flows can be counted as:

- Q_{l1}: leakage between the rotor inner area and the oil chamber due to a clearance, ζ_{l1}:

$$Q_{l1}(\alpha_i, \alpha_{i+1}) = \frac{b\zeta_{l1}^3\left(P(\alpha_i, \alpha_{i+1}) - P_{\min}\right)}{12\eta_{oil}\left(R_r - R_{ri}\right)} \tag{11}$$

here η_{oil} is the dynamic viscosity of oil.

- Q_{l2}: leakage between the rotor inner area and the oil chamber due to a clearance, ζ_{l2}:

$$Q_{l2}(\alpha_i,\alpha_{i+1})=\frac{\left[|\alpha_i-\alpha_{i+1}|R_{ri}-t_v-\zeta_{l1}\right]\zeta_{l2}^3\left(P(\alpha_i,\alpha_{i+1})-P_{\min}\right)}{12\eta_{oil}\left(R_r-R_{ri}\right)} \tag{12}$$

- Q_{l3}: leakage between the rotor inner area and the oil chamber due to a clearance, ζ_{l3}:

$$Q_{l3}(\alpha_i,\alpha_{i+1})=\frac{t_v\zeta_{l3}^3\left(P(\alpha_i,\alpha_{i+1})-P_{\min}\right)}{12\eta_{oil}\left(R_r-R_{ri}\right)} \tag{13}$$

- Q_{l4}: leakage between the oil chamber and its previous chamber due to a clearance, $\zeta_{l4}\equiv\zeta_{l3}$:

$$Q_{l4}(\alpha_i,\alpha_{i+1})=\frac{l_{v(i+1)}\zeta_{l4}^3\left(P(\alpha_{i+1},\alpha_{i+2})-P(\alpha_i,\alpha_{i+1})\right)}{12\eta_{oil}t_v} \tag{14}$$

- Q_{l5}: leakage between the oil chamber and its next chamber due to a clearance, $\zeta_{l5}\equiv\zeta_{l3}$:

$$Q_{l5}(\alpha_i,\alpha_{i+1})=\frac{l_{vi}\zeta_{l5}^3\left(P(\alpha_i,\alpha_{i+1})-P(\alpha_{i-1},\alpha_i)\right)}{12\eta_{oil}t_v} \tag{15}$$

- Q_{l6}: leakage between the oil chamber and the area outside ring due to a clearance, ζ_{l6}:

$$Q_{l6}(\alpha_i,\alpha_{i+1})=\frac{\left[|\alpha_i-\alpha_{i+1}|\frac{\rho_i+\rho_{i+1}}{2}\right]\zeta_{l6}^3\left(P(\alpha_i,\alpha_{i+1})-P_{\min}\right)}{12\eta_{oil}\left(R_{se}-R_s\right)} \tag{16}$$

- Q_{l7}: leakage between the oil chamber and its previous chamber due to a clearance between the vane front side (vane tip) and the ring inner contour.
- Q_{l8} leakage between the oil chamber and its next chamber due to a clearance between the vane tip and the ring inner contour.

During the operation, the vane tip edges contact with the inner contour of the ring in most cases due to the pressurized oil in the chambers under vanes and the centrifugal forces. Since, the leakages, Q_{l7} and Q_{l8}, are neglected. Hence, the total leakage flow of an oil chamber between two consecutive vanes is obtained:

$$\Delta Q_{leak}(\alpha_i,\alpha_{i+1})=2Q_{l4}(\alpha_i,\alpha_{i+1})-\sum_{i=1}^{6}Q_{li}(\alpha_i,\alpha_{i+1}) \tag{17}$$

3.2.2 Power loss due to temperature and pressure changes

For evaluating the effects of temperature and pressure on the pump flow rate, an equivalent laminar flow Q_{eq} of oil through a long cylindrical pipe, with radius R_{eq} and length L_{eq}, is used. The equivalent flow rate can be computed using Poiseuille's equation:

$$Q_{eq}(t)=\frac{\pi}{8}\times\frac{R_{eq}^4}{\eta_{oil}(t)}\times\frac{P_{\max}(t)-P_{\min}}{L_{eq}} \tag{18}$$

$$\eta_{oil}(t)=\upsilon_{oil}(t)\times\rho_{oil}(t) \tag{19}$$

where $\upsilon_{oil}(t)$ is kinematic viscosity of oil; and the oil density is derived from its defined value at time t=0 as

$$\rho_{oil}(t)=\frac{\rho_{oil0}}{\left[1+\lambda_{oil}(T_1-T_0)\right]\left[1-(P_{\max 1}-P_{\max 0})/\beta_{oil}\right]} \tag{20}$$

where λ_{oil} is volumetric temperature expansion coefficient; T_0 - P_{max0} and T_1 - P_{max1} are in turn the initial and final working temperature - pressure.

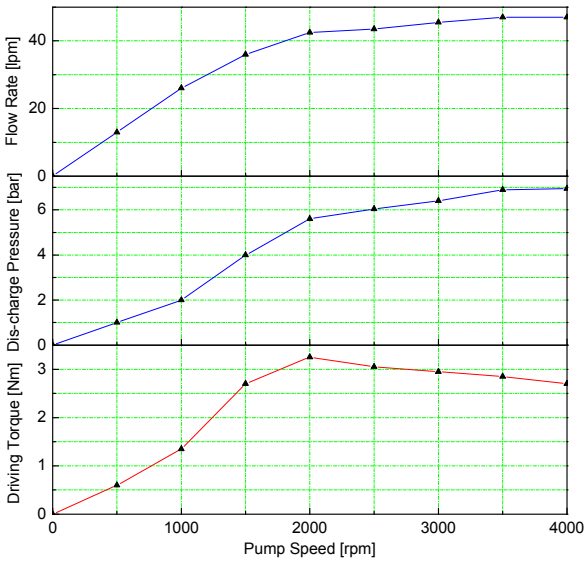

Fig. 8 Actual performance of the researched vane pump

To eliminate the error in evaluating the flow variation due to temperature and pressure changes, only the derivative of flow rate caused by these factors is used as in (21) to evaluate the flow rate loss.

$$\Delta Q_{TP}(t) \equiv \frac{\pi}{8} \times \frac{R_{eq}^4}{L_{eq}} \times \left[\frac{\Delta P(t)}{\eta_{oil}(t)} - \frac{\Delta P(t-1)}{\eta_{oil}(t-1)} \right] \tag{21}$$

3.2.3 Power loss due to friction

In the ideal pump, the driving torque, τ_{th}, without energy loss is derived by

$$\tau_{th} = \frac{D_{th}}{2\pi}(P_{\max} - P_{\min}) \tag{22}$$

where D_{th} is the theoretical displacement of the pump.

$$D_{th} = \frac{Q_{th}}{n} \tag{23}$$

Due to the friction problem, the actual pump driving torque is larger than the ideal torque an amount called friction torque $\Delta\tau$:

$$\Delta\tau = \tau_{act} - \frac{Q_{th}}{n}(P_{\max} - P_{\min}) \tag{24}$$

The friction factors are known as

- Friction between the vane tips and the ring inner contour
- Friction between the pump shaft and oil seals
- Friction between the pump shaft and bearings
- Friction between the ring, rotor and vanes with the pump cover

Among the friction factors mentioned above, only the friction between the vane tips and the ring inner contour is varied correspondingly to the variation of the working pressure and pump speed while the other friction factors can be considered to be constant values during the pump operation (see Fig. 9). The friction force, F_{frv}, between a generic vane and the ring inner contour is computed as

$$F_{frv}(\alpha_i) = \chi\Big[\big(F_{v\_cen}(\alpha_i) + F_{oil\_cen}(\alpha_i) + F_{uv\_oil}(\alpha_i)\big) \times \cos\Delta\alpha_{r/s}(\alpha_i)\Big] \tag{25}$$

where

+ χ is kinetic frictional coefficient between the vane and ring in the lubrication condition.
+ $F_{v\_cen}(\alpha_i)$, and $F_{oil\_cen}(\alpha_i)$ are the centrifugal forces of the vane i^{th}, and the oil chamber under this vane.
+ $F_{uv\_oil}(\alpha_i)$ is caused by the pressurized oil in the chamber under the considered vane:

$$F_{uv\_oil}(\alpha_i) = P(\alpha_i) \times b \times t_v \tag{26}$$

+ $\Delta\alpha_{r/s}(\alpha_i)$ is the angle difference between the direction of forces $F_{v\_cen}(\alpha_i), F_{oil\_cen}(\alpha_i), F_{uv\_oil}(\alpha_i)$ and the direction perpendicular to the tangent of the ring at its contact point with the vane tip:

$$\Delta\alpha_{r/s}(\alpha_i) = \alpha_r(\alpha_i) - \alpha_s(\alpha_i) \tag{27}$$

From (50), the friction torque between a generic vane and the ring inner contour can be calculated as

$$\tau_{frv}(\alpha_i) = F_{frv}(\alpha_i) \times \cos\Delta\alpha_{r/s}(\alpha_i) \times \rho_i \tag{28}$$

Hence, the total friction torque between the vanes and ring inner contour is given:

$$\tau_{frv} = \sum_{i=1}^{N} \tau_{frv}(\alpha_i) \tag{29}$$

In other words, the pump flow rate lost due to this friction factor can be evaluated as

$$\Delta Q_{frv}(t) = n\frac{2\pi\tau_{frv}}{P_{\max} - P_{\min}} \tag{30}$$

Finally, the friction torque added to the driving torque of the pump is derived:

$$\Delta\tau = \tau_{frv} + \tau_{fr0} \tag{31}$$

where τ_{fr0} is constant friction torque which is the sum of friction torques due to: friction between the pump shaft and oil seals/ bearings, and friction between the ring, rotor and vanes with the pump cover. This factor is determined from the actual performance of the pump.

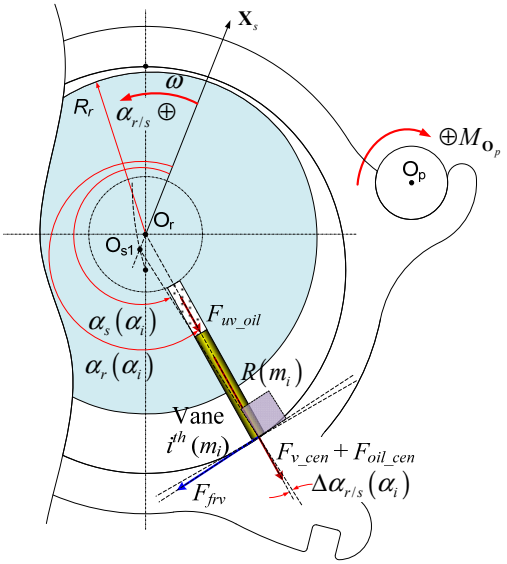

Fig. 9 Analysis of friction force between a generic vane and the ring inner contour

And the total pump flow rate lost due to all the friction factors is computed as

$$\Delta Q_{fric}(t) = \Delta Q_{frv}(t) + \Delta Q_{fr0} \tag{32}$$

where ΔQ_{fr0} is the lost flow corresponding to the constant friction torque τ_{fr0}.

3.2.4 Power loss due to incomplete filling effect

The incomplete filling effect of pumping chambers with oil is normally as a function of excessive flow restriction in the flow path to the pump at a specific rotation speed.

The probability of this incomplete filling effect increases with higher rotational speed of the pump. In the ideal working condition, the pumping chambers have enough time to fill their volumes before connecting to the delivering port, subsequently generating the pressurized oil as described in Section 2.2.2. On the contrary, in defective filling condition – at high working speeds, the large amount of fluid is proportionally passed through the feed ducts and intake valves of the system. For a constant fluid pressure at the pump intake, a certain critical speed exists where the amount of fluid required to fill the working chambers cannot enter to the pump at the intake. Therefore by further increasing the speed above this critical value, a proportional increase in pump delivery will not occur, or the pump flow rate may even decrease. This problem is remarkable when the pump works at high speed region.

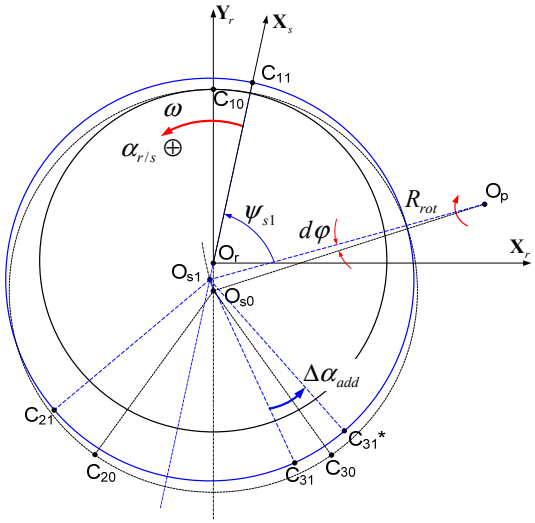

Fig. 10 Pressure re distribution due to incomplete filling effect

In addition, when the working chambers connect with the delivering port, oil amounts from this port enter into the chamber vacancies. This undesirably entranced oil is called backflow of oil. It causes the pressure within each chamber to do not increase until the chamber becomes filled after an additional rotation of the rotor. The additional rotation angle is represented by $\Delta\alpha_{add}$. The pressure distribution analyzed in Section 2.2.2 and Fig. 3 was then adjusted as presented in Fig. 10. Hence, the total moment acting on the ring caused by the pressurized oil inside the ring in (3) becomes:

$$\begin{aligned}\sum M_{O_{p\_oil\_inside}} &= \int_0^{\alpha_{C2t}} R_{rot}\sin(\psi_{st}+\alpha_s)P_{\min}bR_s d\alpha_s \\ &+ \int_{\alpha_{C2t}}^{\alpha_{C3t}^H} R_{rot}\sin(\psi_{st}+\alpha_s)f(P)bR_s d\alpha_s \\ &+ \int_{\alpha_{C3t}^L}^{2\pi} R_{rot}\sin(\psi_{st}+\alpha_s)P_{\max}bR_s d\alpha_s \\ f(P) &= \left[(P_{\max}-P_{\min})\frac{\alpha_s-\alpha_{C2t}}{\alpha_{C3t}-\alpha_{C2t}}+P_{\min}\right] \\ \alpha_{C3t}^H &= \alpha_{C3t}+\Delta\alpha_{add};\ \alpha_{C3t}^L = \alpha_{C3t}-\Delta\alpha_{add}\end{aligned} \tag{33}$$

Due to the pressure re distribution, it makes

the ring be easier to be rotated around the pivot in the direction that reduces the eccentricity between the rotor and the ring. In other words, the pump displacement is also reduced in this situation.

It can be point out that the incomplete filling effect cause a reduction, ΔQ_{fill}, of the pump flow rate which may be proportional to the rotational speed. The higher working speed, the large value of the additional angle $\Delta\alpha_{add}$ and the large amount of lost flow are obtained. Hence, to determine this pump flow reduction, the tendency of the additional angle $\Delta\alpha_{add}$ is determined by using a comparison between the theoretical flow rate and the actual flow rate and iterative method.

From all the above analyses, an estimation of the actual pump flow rate can be established in (34).

$$Q_{est} = Q_{th} + \Delta Q_{leak} + \Delta Q_{TP} - \Delta Q_{fric} - \Delta Q_{fill} \quad (34)$$

4. Estimation of actual pump performance using the complete model

In order to estimate the actual pump flow rate, simulations with the complete pump model based on the power loss analysis have been performed with the same testing conditions set for the experiments (Section 3.1). The parameters set for the complete model are displayed in Table 1.

Component	Factor	Unit	Value
Pump design clearances	ζ_{l1}	mm	0.3
	ζ_{l2}	mm	0.14
	$\zeta_{l3} \equiv \zeta_{l4} \equiv \zeta_{l5}$	mm	0.17
	ζ_{l6}	mm	0.1
Lubrication oil – SAE 5W-20	β_{oil}	N/m^2	1.5×10^9
	ρ_{oil} at 15°C	kg/m^3	852
	λ_{oil}	1/°C	6.4×10^{-4}
	υ_{oil} at [-30; 40; 100; 120] °C	mm^2/s	[4200; 47; 8.9; 5.91]
Vanes and ring	χ at 1000rpm [16]	-	0.1064

By employing the power loss analysis presented above, the fitted curve of the additional angle caused by the incomplete filling effect was found as shown in Fig. 11 in a comparison with the set of this angle approximated using the linear interpolation. It can be seen that this angle was mostly varied proportionally with the pump speed. As the result, the estimated and actual pump performances were obtained and compared as plotted in Fig. 12 while the power loss was analyzed in Fig. 13. As seen in Fig. 13, the power losses were remarkable, especially at high working speeds of the pump. Most of the lost energy was due to the friction and leakage problems. The results point out that the complete model not only could show the theoretical pump flow rate but also could analyze well most of the power loss factors then, consequently, brings to the accurate estimation of actual pump flow.

However, Fig. 11 points out that, the slope of the additional angle trajectory actually tended to be smaller values at higher pump speeds. It was due to the reduction of the pump eccentricity which, consequently, reduces the pump compression ratio as well as the cavitation and aeration levels. In addition, the other small power loss factors such as leakages caused by clearance variations due to temperature and/or surface finish condition changes, etc, were not considered in this study. As a result, the predicted pump performance

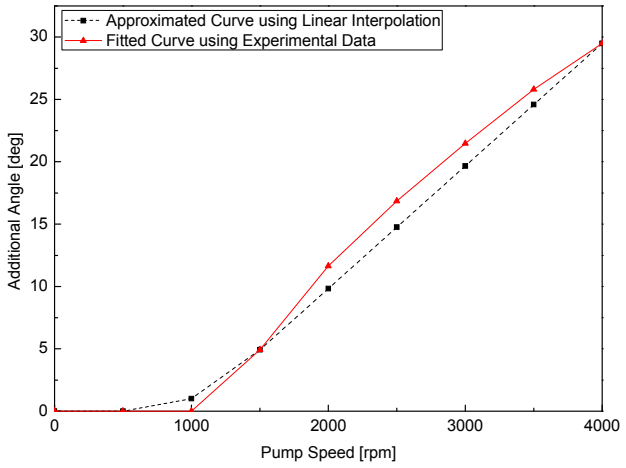

Fig. 11 Comparison of fitted and approximated curves of the additional angle

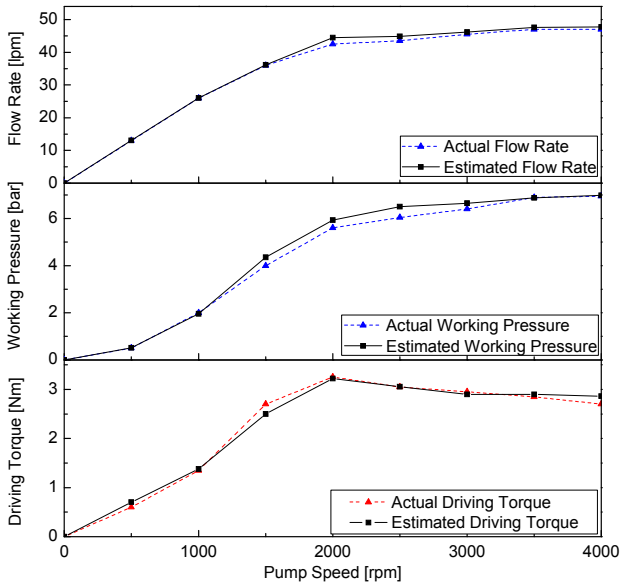

Fig. 12 Comparison of actual and estimated pump performances

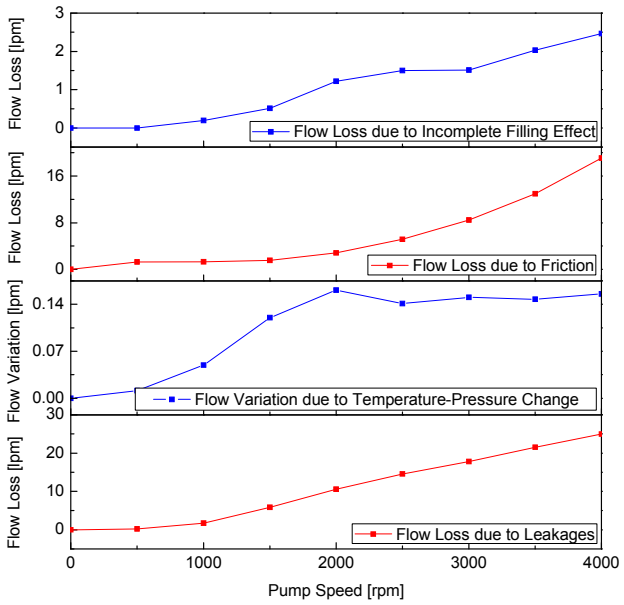

Fig. 13 Power loss analysis for the pump

was not much fit with the actual performance at some working conditions (Fig. 12 and Fig. 13). Hence, a better representation of the additional angle trajectory as well as further investigations on other loss factors can bring to a higher accuracy in estimating the actual pump performance.

5. Conclusions

The advanced technology for lubrication system using the variable displacement vane-type oil pump is introduced in this paper. By employing the displacement control mechanism based on the working pressure and the balance spring, the lubricating oil can be easily and continuously adjusted with respect to the desired performance to obtain the highest lubricating efficiency. A variable displacement vane-type oil pump made by MyungHwa Co. Ltd. has been investigated. Firstly, the theoretical model of this pump was revised. Secondly, the power loss analysis for this pump has been carried out to construct the complete and accurate pump model.

Numerical simulations have been carried out in the comparison with the experiments to investigate and verify the working performance of the complete pump model. The comparison results prove that the complete pump model could estimate well the power loss factors. As a result, the actual pump performance could be predicted with high accuracy by using this model. This variable displacement vane-type oil pump and it developed model may become an advanced solution for industrial machines with lubrication purpose in the near future.

Acknowledgements

This research was financially supported by the Ministry of Education, Science Technology (MEST) and National Research Foundation of Korea (NRF) through the Human Resource Training Project for Regional Innovation.

References

1) Rexroth variable displacement vane-type oil pump - http://www.bosch Rexroth.com
2) Atos variable displacement vane-type oil pump - http://www.atos.com
3) Scoda variable displacement vane-type oil pump - http://www.scoda.it
4) Magna Powertrain Inc., Continuously variable displacement vane pump and system, Patent No.: WO 2007/128106 A1, 2007.

5) Magna Powertrain Inc., Variable Capacity vane pump with force reducing chamber on displacement ring, Patent No.: US 2009/0074598 A1, 2009.
6) Magna Powertrain Inc., Variable capacity vane pump with dual control chambers, Patent No.: US 7794217 B2, 2010.
7) D.R. Staley and B.K. Pryor, Pressure regulating variable displacement vane pump, Patent No.: US 7862306 B2, 2011.
8) A. Giuffrida and R. Lanzafame, "Cam shape and theoretical flow rate in balanced vane pumps," Mechanism and Machine Theory, Vol. 40, pp. 353-369, 2005.
9) D.R. Staley, B.K. Pryor and K. Gilgenbach, "Adaptation of a Variable Displacement Vane Pump to Engine Lube Oil Applications," SAE Technical Paper 2007-01-1567, pp. 1-9, 2007.
10) S. Loganathan, S. Govindarajan, J.S. Kumar, K. Vijayakumar and K. Srinivasan, "Design and Development of Vane Type Variable flow Oil Pump for Automotive Application," SAE Technical Paper 2011-28-0102, pp. 1-7, 2011.
11) C. Kim, D.Q. Truong, N.T. Trung, K.K. Ahn, J.I. Yoon, J.S. Lee, H.S. Han and J.B. Kim, "Development of an Electronic Control Variable Displacement Lubrication Oil Pump," Proc. of the 15th International Conference on Mechatronics Technology, Melbourne, Australia, paper 65, 2011.
12) MyungHwa variable displacement vane-type oil pump - http://www.myunghwa.com/
13) D.Q. Truong, K.K. Ahn, J.I. Yoon and J.S. Lee, “Development of a mathematic model for a variable displacement vane pump for engine oil,” J. Korean Soc. Fluid Power Constr. Equip., vol. 9, no. 4, pp. 42-51, 2012.